Superlattices and Microstructures 57 (2013) 51–57

Contents lists available at SciVerse ScienceDirect

Superlattices and Microstructures

journal homepage: www.elsevier.com/locate/superlattices

Improved light reflectance and thermal stability of Ag-based ohmic contacts on p-type GaN with La additive

I-Chen Chen [a,*], Bo-Yuan Cheng [a], Wen-Cheng Ke [b], Cheng-Huang Kuo [c], Li-Chuan Chang [d]

[a] *Institute of Materials Science and Engineering, National Central University, Jhongli 320, Taiwan*
[b] *Department of Mechanical Engineering, Yuan Ze University, Jhongli 320, Taiwan*
[c] *Institute of Lighting and Energy Photonics, National Chiao Tung University, Tainan County 711, Taiwan*
[d] *Department of Optics and Photonics, National Central University, Jhongli 320, Taiwan*

ARTICLE INFO

Article history:
Received 20 September 2012
Received in revised form 12 December 2012
Accepted 1 February 2013
Available online 13 February 2013

Keywords:
Ohmic contact
La additive
Light reflectance
Specific contact resistivity

ABSTRACT

We investigated the effect of La additive on the improvement of light reflectance and thermal stability of Ag contacts on p-GaN. A high reflectance of over 90% at 460 nm wavelength and low specific contact resistivity of $5.5 \times 10^{-5}\ \Omega\ \mathrm{cm}^2$ were obtained from La-containing Ag contacts annealed at 300 °C for 1 min, which also show better thermal stability than Ag contacts after annealing in air ambient. The experimental results reveal that the addition of La could effectively slow down Ag migration in $\langle 1\,1\,1\rangle$ direction during annealing, and thus suppress the Ag agglomeration at elevated temperature, leading to a good ohmic contact with improved high reflectance and thermal stability.

1. Introduction

GaN-based vertical-structure light emitting diodes (VLEDs) have drawn much attention due to their high light-extraction efficiency and better thermal dissipation, which make them a promising choice for high power/brightness applications [1–3]. Since emitted light from active regions is reflected up from the contact electrodes on p-GaN in the VLEDs, a high reflectance and low resistance p-GaN ohmic contact is essential to increase the light extraction and improve device performance. Silver (Ag) is a well-known highly reflective metal across the visible spectrum and has been used

---

[*] Corresponding author. Tel.: +886 3 4227151x34907; fax: +886 3 280 5034.
E-mail address: ichen@ncu.edu.tw (I-Chen Chen).

0749-6036/$ - see front matter © 2013 Elsevier Ltd. All rights reserved.
http://dx.doi.org/10.1016/j.spmi.2013.02.002

for ohmic contacts to p-GaN by annealing in air ambient [4–6]. The ohmic behavior could be attributed to the reduction of the Schottky barrier height caused by the formation of Ag–Ga solid solution at the interface between Ag and p-GaN [4]. However, the poor thermal stability of Ag on p-GaN causes film agglomeration during annealing, leading to degradation in electrical and optical properties [4,5]. Therefore, pure Ag films are not suitable to be used as p-GaN contacts for high-power VLEDs.

Regarding the physical origin of Ag agglomeration, two different mechanisms have been suggested, including surface diffusion to reduce the total free energy and bulk diffusion of Ag atoms by oxygen–vacancy interaction [7,8]. The capping layers on the top of Ag films, such as Ru, Mg, La, Zn and NiZn alloy, have been investigated, and proved to be able to reduce film agglomeration and thus result in better thermal stability due to suppression of excessive incorporation of oxygen into the Ag layers [5,9–12]. Furthermore, different Ag alloys, such as Ag–Al, Ag–Cu and Ag–Mg alloys, have been demonstrated to improve the thermal stability of Ag films [6,13–15]. In this letter, we present a new Ag–La metallization scheme for p-GaN ohmic contacts. By adding La additive to Ag contacts, light reflectance and thermal stability of the contacts are improved significantly.

2. Experimental

To investigate the properties of Ag–La contact layers, 1 μm-thick Mg-doped GaN films grown on *c*-plane sapphire substrates using metalorganic chemical vapor deposition were used. The carrier concentration of p-GaN samples determined by Hall measurements is about $5 \times 10^{17}\ \text{cm}^{-3}$. The circular transfer length method (CTLM) was used for specific contact resistivity measurements. The CTLM pattern defined by standard photolithography has a constant outer radius of 200 μm and the gap spacing between the inner and outer pads is varied from 5 to 45 μm. Prior to lithographic patterning process, the as-grown GaN samples were ultrasonically degreased using acetone, methanol and then rinsed in deionized water. In order to remove the surface oxide layer, all samples were dipped into a buffer oxide etch (BOE) solution for 20 min and then placed into the deposition chamber for metallization. 125 nm-thick Ag–La contact patterns were deposited on p-GaN substrates by electron-beam evaporation followed by the lift-off process. In order to make a uniform Ag–La source, we used the vacuum arc melting method. The as-deposited Ag–La film contains 0.6 wt.% La, determined using inductively coupled plasma mass spectrometry. For comparison, a Ag film with the same thickness was also deposited on p-GaN as a reference. The CTLM contacts were then annealed at temperatures ranging from 200 to 450 °C for 1 min in air ambient using a rapid thermal annealing system. The surface morphology and microstructure of Ag and Ag–La films were analyzed by scanning electron microscopy (SEM) and high resolution X-ray diffraction (HRXRD). Current–voltage characteristics of the contacts were examined using a semiconductor parameter analyzer (HP 4145). A UV/Vis/NIR spectrometer (JASCO V-670) was used to measure the reflectance of the Ag and Ag–La contacts deposited on quartz glass.

3. Results and discussion

Fig. 1a shows the specific contact resistivities of Ag and Ag–La contacts as a function of the annealing temperature. Both as-deposited metal contacts on p-GaN exhibit non-ohmic behavior. The specific contact resistivity were calculated for the Ag and Ag–La contacts which reveal ohmic property after annealing at temperature ranges of 200– 400 °C and 200–450 °C, respectively. While the specific contact resistivities of both contacts are similar after annealing at 200 °C, the Ag contact shows a lowest specific contact resistivity of $5 \times 10^{-4}\ \Omega\,\text{cm}^2$ after annealing at 300 °C, where the specific contact resistivity of the Ag–La contact ($5.5 \times 10^{-5}\ \Omega\,\text{cm}^2$) is about one order lower than that of the annealed Ag contact. The specific contact resistivities of Ag and Ag–La contacts dramatically increases at annealing temperatures higher than 400 °C and 450 °C respectively, which implies degradation of the contacts. Fig. 1b shows the reflectance of both contacts at the wavelength of 460 nm as a function of the annealing temperature. Both as-deposited Ag and Ag–La contacts reveal the same reflectance close to 95%. The reflectance of the Ag contact degrades to 80% after annealing at 300 °C and drops quickly with increasing the annealing temperature. Meanwhile, the reflectance of the Ag–La contact is kept over 90% after annealing at 300 °C and degrades slowly over all annealing temperatures, compared

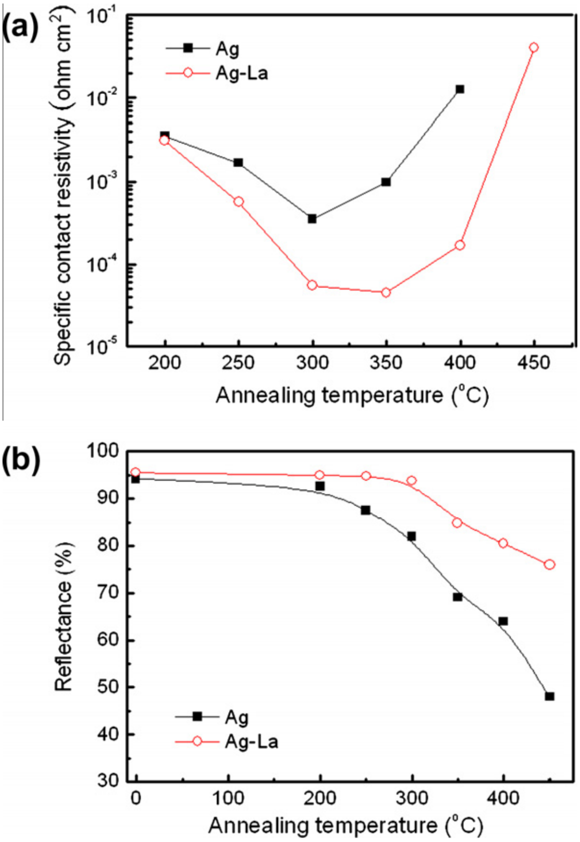

Fig. 1. (a) Specific contact resistance of Ag and Ag–La contacts as a function of annealing temperature in air ambient. (b) Light reflectance at 460 nm wavelength obtained from Ag and Ag–La contacts as a function of annealing temperature in air ambient.

with the Ag contact. The reflectance at 460 nm was chosen for the evaluation of light reflectance since the emission wavelength of GaN LEDs for lighting applications is around that region of the spectrum.

In order to evaluate the thermal stability of both Ag and Ag–La contacts, we investigated the change of specific contact resistivity and light reflectance as a function of annealing time at 250 °C. For easier comparison of the results, the specific contact resistivity of each sample was normalized with its initial contact resistivity (ρ_o) obtained after annealing at 300 °C for 1 min and plotted as (ρ_t/ρ_o) against annealing time, shown in Fig. 2. For the Ag contact, the value of ρ_t/ρ_o is drastically increased by a factor greater than 100 after annealing for 60 min. Meanwhile, the specific contact resistivity of the Ag–La contact is only about five times greater than its initial value after annealing for 120 min. The light reflectance of the Ag contact decreases to 60% after annealing at 250 °C for 45 min, while the reflectance of the Ag–La contact shows high reflectance of 80%. These results in Figs. 1 and 2 indicate that the La additive could suppress the degradation of the Ag–La contact and thus result in better thermal stability.

The surface morphology of as-grown Ag films is similar to that of the Ag–La films, as shown in Fig. 3a and b. After annealing at 300 °C in air ambient, however, the annealed Ag contact shows a very irregular and isolated hole morphology (shown in Fig. 3c), which could be explained on the basis of the high surface diffusion of Ag atoms in the oxygen-contained ambient [16]. The hole formation in Ag films is enhanced in the presence of oxygen and thus leads to Ag agglomeration, which would strongly reduce the contact area and, thus result in a poor specific contact resistivity and a low light reflectance,

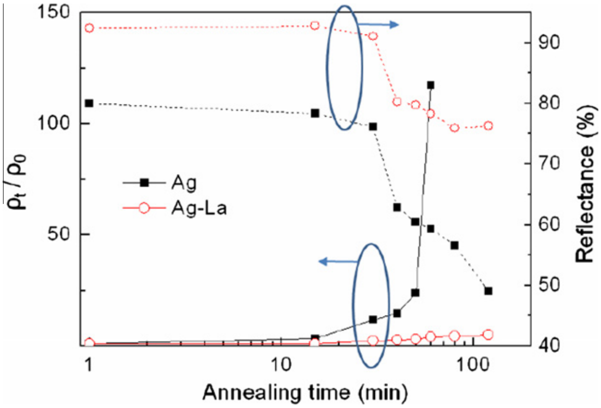

Fig. 2. Comparison of ρ_t/ρ_o ratios for Ag and Ag–La contacts as a function of annealing time at 250 °C in air ambient.

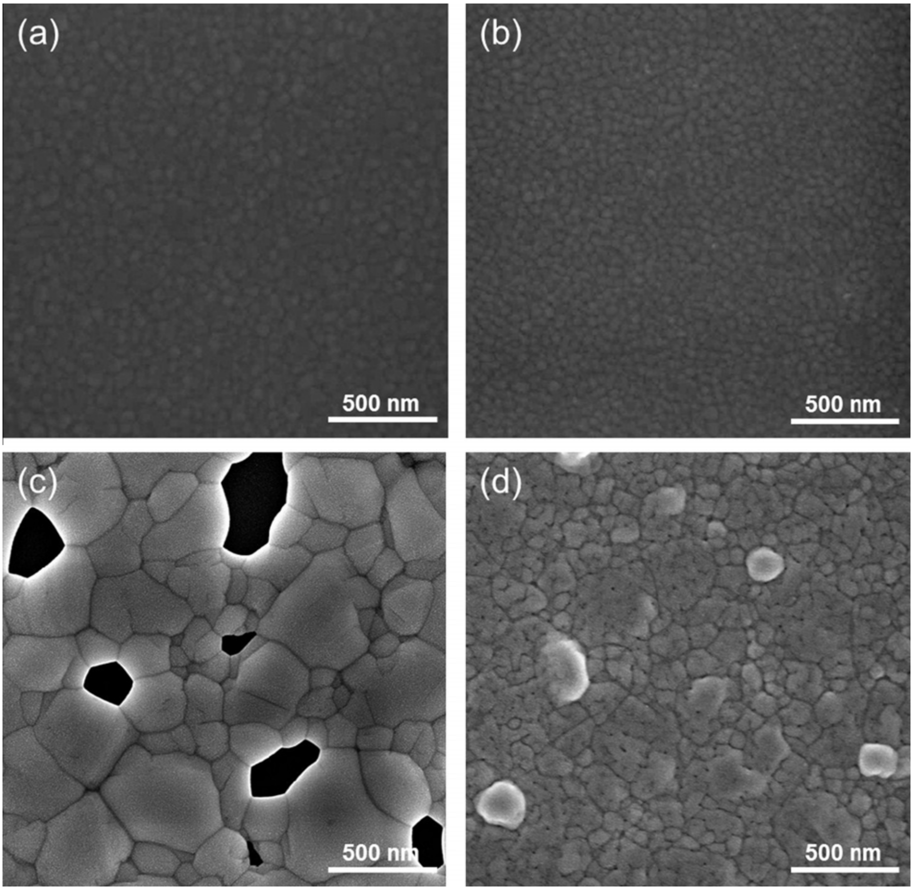

Fig. 3. SEM images of (a) an as-deposited Ag film, (b) an as-deposited Ag–La film, (c) a Ag film annealed at 300 °C for 1 min in air and (d) a Ag–La film annealed at 300 °C for 1 min in air.

as indicated in Fig. 1. Contrary to the Ag contact, no holes are found in the Ag–La sample after annealing under the same condition although the surface roughness is a little increased, as shown in Fig. 3d.

In order to investigate the interfacial reactions between metal contacts and GaN, secondary ion mass spectrometry (SIMS) depth profiles were obtained from both contacts before and after annealing, as shown in Fig. 4. The interdiffusion of contact metal and GaN during annealing leads to the formation of Ag–Ga solid solution, which produces acceptor-like Ga vacancies beneath the contact, resulting in the reduction of the Schottky barrier height [17]. For the Ag contact, as depicted in Fig. 4a and b, Ga atoms significantly outdiffuse to the surface of the annealed Ag contact. Meanwhile, for the Ag–La contact, it is observed that a thin La-rich alloy layer exists near the p-GaN interface for the as-deposited sample, as shown in Fig. 4c. This indicates that the La atoms tend to evaporate from the premixed Ag–La source in the early stage of film deposition. After thermal annealing, the La profile coincides with the Ag profile, implying that the La atoms are uniformly distributed in the whole contact layer. Comparing Fig. 4b and d, the outdiffusion of Ga atoms in annealed Ag–La contacts is found to be much less serious than that in annealed Ag contacts. Since Ga outdiffusion could be enhanced by annealing in the oxygen-contained ambient due to the high reactivity of Ga with oxygen [18], we speculate that excessive oxygen could be prevented from diffusing into GaN during annealing due to the suppression of Ag agglomeration in Ag–La contact by La additive.

For reduction of the free energy of the system, agglomeration of polycrystalline films occurs by atomic diffusion, and causes dewetting of metallic films, resulting in a partly uncovered substrate surface and irregular film morphology. From the previous study [6], it is pointed out that crystal grains of Ag films tend to be ⟨1 1 1⟩-oriented to minimize the surface energy of the films during thermal annealing. Ag atoms in other textured grains migrate and merge into growing {1 1 1} grains, leading to the

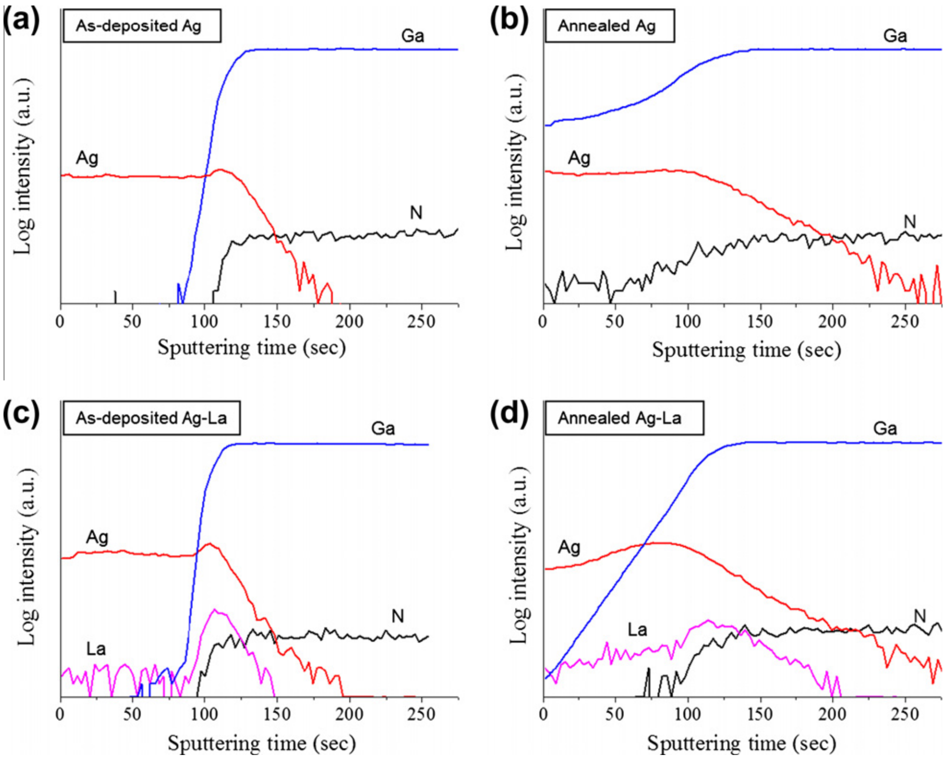

Fig. 4. SIMS depth profiles of Ag and Ag–La contacts before and after annealing at 300 °C. Both contacts were annealed under air atmosphere for 1 min.

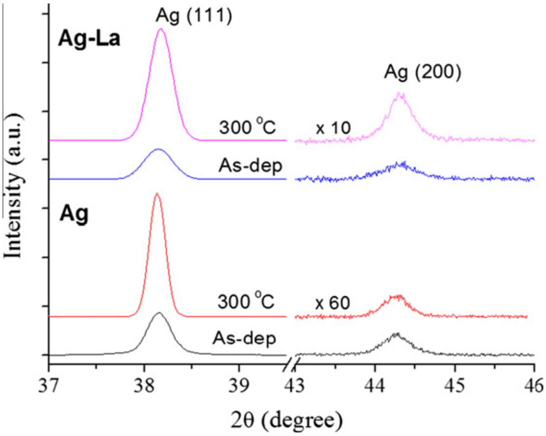

Fig. 5. HRXRD θ–2θ profiles of Ag and Ag–La films before and after annealing at 300 °C.

formation of voids and finally the isolated Ag islands. Fig. 5 shows HRXRD θ–2θ scans of the pure Ag and Ag–La films before and after annealing at 300 °C. The change in XRD peak intensities of Ag (1 1 1) and (2 0 0) were investigated. For the as-deposited films, the intensity ratio of $I_{(111)}/I_{(200)}$ (=76.9) in the Ag contact is much higher than that (=6.3) of the Ag–La sample. However, the value of $I_{(111)}/I_{(200)}$ is increased up to 250 for the Ag contact after annealing at 300 °C. Meanwhile, the intensity ratio of $I_{(111)}/I_{(200)}$ in the annealed Ag film is kept around 8.8, indicating that La additive could efficiently reduce the diffusion of Ag atoms to Ag (1 1 1) planes and thus enhance the resistance to Ag agglomeration. In addition, the SEM images in Fig. 3c and d shows that the grain sizes of the annealed Ag–La contact are smaller than those of the annealed Ag contact, which imply that the grain migration is retarded in annealed Ag–La films, resulting in the suppression of agglomeration. The improvement in the specific contact resistance and light reflectance for the Ag–La contact is speculated due to less reduction of the contact area during annealing.

4. Conclusion

In summary, a highly reflective and low resistance Ag–La ohmic contact for p-GaN has been demonstrated. The Ag–La contact shows a low specific contact resistance of $5.5 \times 10^{-5}\ \Omega\,\mathrm{cm}^2$ and high relative reflectance of over 90% after annealing at 300 °C in air. We suggest that La additive could effectively prohibit Ag–La films from evolving into $\langle 1\,1\,1\rangle$-preferred orientation during annealing and thus suppress the Ag agglomeration. The results indicate that the Ag–La film has potential for applications of p-GaN contact in VLEDs.

Acknowledgment

This research was supported by National Science Council of Taiwan under Grant Nos. 100-2221-E-008-053 and 101-2221-E-008-041.

References

[1] T. Fujii, Y. Gao, R. Sharma, E.L. Hu, S.P. DenBaars, S. Nakamura, Appl. Phys. Lett. 84 (2004) 855–857.
[2] S.-J. Wang, K.-M. Uang, S.-L. Chen, Y.-C. Yang, S.-C. Chang, T.-M. Chen, C.-H. Chen, Appl. Phys. Lett. 87 (2005) 011111.
[3] O.B. Shchekin, J.E. Epler, T.A. Trottier, T. Margalith, D.A. Steigerwald, M.O. Holcomb, P.S. Martin, M.R. Krames, Appl. Phys. Lett. 89 (2006) 071109.
[4] J.-O. Song, J.S. Kwak, Y. Park, T.-Y. Seong, Appl. Phys. Lett. 86 (2005) 062104.
[5] J.-S. Park, J.-W. Jeon, C.-H. Lee, C.-H. Choi, S. Jin, T.-Y. Seong, Superlattice Microstruct. 52 (2012) 357–363.
[6] J.-Y. Kim, S.-I. Na, G.-Y. Ha, M.-K. Kwon, I.-K. Park, J.-H. Lim, S.-J. Park, Appl. Phys. Lett. 88 (2006) 043507.

[7] H.C. Kim, N.D. Theodore, T.L. Alford, J. Appl. Phys. 95 (2004) 5180–5188.
[8] J.-P. Crocombette, H. Monestrol, F. Willaime, Phys. Rev. B 66 (2002) 024114.
[9] H.W. Jang, J.H. Son, J.-L. Lee, Appl. Phys. Lett. 90 (2007) 012106.
[10] I.-C. Chen, Y.-D. Chen, C.-C. Hsieh, C.-H. Kuo, L.-C. Chang, J. Electrochem. Soc. 158 (2011) H285–288.
[11] J.-S. Park, J.-W. Jeon, S. Jin, T.-Y. Seong, Electrochem. Solid-State Lett. 15 (2012) H130–132.
[12] S. Jung, Y.-H. Kim, J.-H. Oh, T.-Y. Seong, Superlattice Microstruct. 46 (2009) 578–584.
[13] J.H. Son, G.H. Jung, J.-L. Lee, Appl. Phys. Lett. 93 (2008) 012102.
[14] Y.H. Song, J.H. Son, G.H. Jung, J.-L. Lee, Electrochem. Solid-State Lett. 13 (2010) H173–H175.
[15] R. Kawai, T. Mori, W. Ochiai, A. Suzuki, M. Iwaya, H. Amano, S. Kamiyama, I. Akasaki, Phys. Status Solidi C 6 (2009) S830–S832.
[16] S.K. Sharma, J. Spitz, Thin Solid Films 65 (1980) 339–350.
[17] H.W. Jang, J.-L. Lee, Appl. Phys. Lett. 85 (2004) 5920–5922.
[18] H.W. Jang, S.Y. Kim, J.-L. Lee, J. Appl. Phys. 94 (2003) 1748–1750.